Density-profile steepening by laser radiation in a magnetized inhomogeneous plasma

Zhi-zhan Xu, Jian Yu, and Yong-hong Tang
Shanghai Institute of Optics and Fine Mechanics, Academia Sinica, P.O. Box 8211, Shanghai, People's Republic of China
(Received 28 May 1985)

The effects of a self-generated magnetic field on the density-profile modification in laser-plasma interactions are investigated by means of calculating the field structure with the assumption of plane electromagnetic waves propagating into a one-dimensional inhomogeneous magnetized plasma. The computed results are in good agreement not only with laser-target experiments using a Nd-glass laser, but also with those using a CO_2 laser. In addition, the calculations give the density dip also observed in experiments.

I. INTRODUCTION

In laser-plasma interactions, the profile of plasma-density distribution plays an important role in the propagation and absorption of an electromagnetic wave in the plasma.[1,2] Experiments using high-intensity lasers demonstrated the phenomenon of plasma-density-profile steepening, which is closely connected with the effects of ponderomotive force. It is noteworthy that the plasma-density-profile steepening depends on the wavelength of the incident laser. In experiments with a Nd-glass laser ($\lambda=1.06$ μm), the density-profile steepening appears only when the intensity of laser light is above 10^{14} W/cm^2, and the observed upper-shelf density is never above $10n_{cr}$,[3,4] where n_{cr} is the critical density while in experiments with CO_2 lasers ($\lambda=10.6$ μm) the density-profile steepening can be seen at light intensity of only about 10^{13} W/cm^2, and the upper-shelf density can reach $40n_{cr}$ and above.[5] There even exists indirect evidence of observing an upper-shelf density of $400n_{cr}$.[6] In addition, the density dip near the critical-density surface is observed in both CO_2 and Nd-glass laser-target experiments. The theories currently available describing the modification of plasma-density profile are all based on the assumption of nonmagnetized plasma.[7-10] Their predictions, though compatible with some observations of Nd-glass laser experiments, are inconsistent with the experiments using a CO_2 laser. In view of there being a large self-generated magnetic field, Fedosejevs *et al.*[5] have suggested the effects of a self-generated magnetic field on the supercritical density profile, but no further work on this subject has appeared. In this paper we start from the theoretical model of laser light normally incident on a one-dimensional inhomogeneous magnetized plasma, by calculating the structure of the electromagnetic field, and we discuss the effects of a self-generated magnetic field on the plasma-density modification. Our results agree not only with those of Nd-glass laser experiments, but also with those of CO_2 laser experiments. In addition, the density dip structure observed in the vicinity of the critical surface is also a natural consequence of our theoretical work.

II. ELECTROMAGNETIC FIELD STRUCTURE

Consider a plane electromagnetic wave $\mathbf{E}_L=\mathbf{E}_L e^{i(\mathbf{k}\cdot\mathbf{r}-\omega t)}$ propagating from a vacuum into a one-dimensional inhomogeneous plasma with density gradient ∇n in the x direction. If there is no external magnetic field, the electromagnetic wave propagating into a plasma only consists of the ordinary mode, which gives no resonance. If there exists a constant magnetic field B_0 in the z direction, the electron motion under the action of Lorentz's force causes the electric vector of the incident wave to change direction, and hence introduces a component of E_x which can couple with the inherent oscillation of the plasma.[11,12] In real physical processes, the self-generated dc magnetic field in laser-plasma interactions can act as the above-mentioned constant magnetic field B_0.

The above noted process can be readily described by using Maxwell's equations and the fluid equations. Electromagnetic waves propagating into a plasma satisfy the wave equation derived from Maxwell's equations,

$$\nabla(\nabla\cdot\mathbf{E})-\nabla^2\mathbf{E}-\frac{\omega^2}{c^2}\mathbf{E}=-\frac{4\pi\omega ne\mathbf{u}}{c^2}\ , \tag{1}$$

where n is the plasma density, ω the laser frequency, and $\mathbf{u}$ the quiver velocity of an electron in the driving field of the laser light. $\mathbf{u}$ can be given in the following equation:

$$m_e\frac{d\mathbf{u}}{dt}=e\left[\mathbf{E}+\frac{1}{c}\mathbf{u}\times\mathbf{B}_0\right]-\nu m_e\mathbf{u}\ , \tag{2}$$

where m_e is the mass of the electron and ν is the damping rate. Substituting $\mathbf{u}$ obtained from (2) into (1), and noticing that the inhomogeneity of plasma is only in the x direction, we have

$$(k_y^2+k_z^2-k_0^2)E_x+i\frac{\partial}{\partial x}(k_yE_y)+i\frac{\partial}{\partial x}(k_zE_z)$$
$$-i\frac{k_0^2\omega_p^2(\nu-i\omega)E_x}{\omega[(\nu-i\omega)^2+\omega_c^2]}+i\frac{k_0^2\omega_p^2\omega_cE_y}{\omega[(\nu-i\omega)^2+\omega_c^2]}=0\ , \tag{3a}$$

$$(k_z^2-k_0^2)E_y+i\frac{\partial}{\partial x}(k_yE_x)+k_yk_zE_z-\frac{\partial^2}{\partial x^2}E_y$$
$$-i\frac{k_0^2\omega_p^2\omega_cE_x}{\omega[(\nu-i\omega)^2+\omega_c^2]}-i\frac{k_0^2\omega_p^2(\nu-i\omega)E_y}{\omega[(\nu-i\omega)^2+\omega_c^2]}=0\ , \quad (3b)$$

$$(k_y^2-k_0^2)E_z-\frac{\partial^2}{\partial x^2}E_z-k_yk_zE_y+i\frac{\partial}{\partial x}(k_zE_x)$$
$$-i\frac{k_0^2\omega_p^2E_z}{\omega(\nu-i\omega)}=0\ , \quad (3c)$$

where $\omega_p=(4\pi ne^2/m_e)^{1/2}$ is the local frequency of plasma, $\omega_c=eB_0/m_ec$ is the electron cyclotron frequency, k_x,k_y,k_z are the components of the wave-number vector, and $k_0^2=k_x^2+k_y^2+k_z^2$. Since we deal with the case of normal incidence only, we can substitute $k_y=k_z=0$ into the above equations. If we write all equations in the dimensionless form, i.e., $N=\omega_p^2/\omega^2$, $\xi=k_0x$, $f=\nu/\omega$, $\alpha=\omega_c^2/\omega^2$, $A=E/E_L$, after some simple algebraic calculations Eq. (3) can be written as

$$A_x=\frac{iN\sqrt{\alpha}A_y}{(\alpha+N+f^2-1)+if(N-2)}\ , \quad (4a)$$

$$\frac{\partial^2A_z}{\partial\xi^2}+\left[1+\frac{N[(N-1)(1-\alpha-N)-f^2]+ifN(\alpha+f^2+N-1)}{(N+\alpha+f^2-1)^2+f^2(N-2)^2}\right]A_y=0\ , \quad (4b)$$

$$\frac{\partial^2A_z}{\partial\xi^2}+i\frac{NA_z}{f-i}+k_0^2A_z=0\ . \quad (4c)$$

Apparently, the dc magnetic field only affects the behavior of electric field components A_x and A_y, and A_z remains unchanged. The coupling between A_x and A_y forms the extraordinary mode in a magnetized plasma, while A_z is still the ordinary mode. Since we are interested only in the influence of self-generated magnetic fields on the laser-plasma interaction, we will omit discussion of A_z.

Assuming an initial linear density profile, we can solve Eq. (4b). The imaginary part in the equation can be neglected because the parameter f is usually very small. The boundary conditions can be easily obtained from physical considerations; i.e., freely outgoing waves at the vacuum side and evanescent waves at the high-density side.

After A_y is deduced by numerical method from Eq. (4b), A_x can be directly calculated from Eq. (4a). In this way, we obtained the structure of an electromagnetic field over the whole coronal region. In particular, we have in-

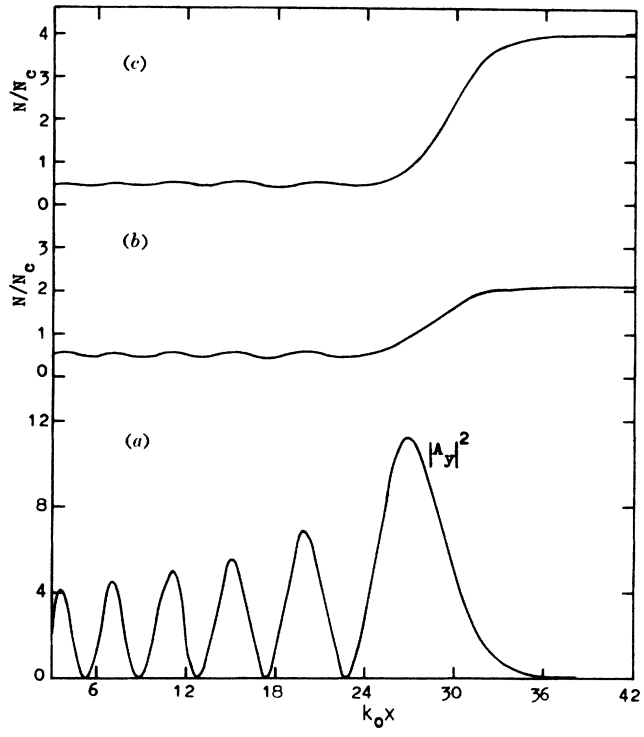

FIG. 1. The field structure and density profile for $\xi=k_0L=30$, $\alpha=0$, $f=0$, where L is the scale length of the initial linear density profile. (a) Field structure, the light wave in a vacuum has amplitude $A=1$. (b) Density profile for $v_0/v_e=0.4$. (c) Density profile for $v_0/v_e=0.6$.

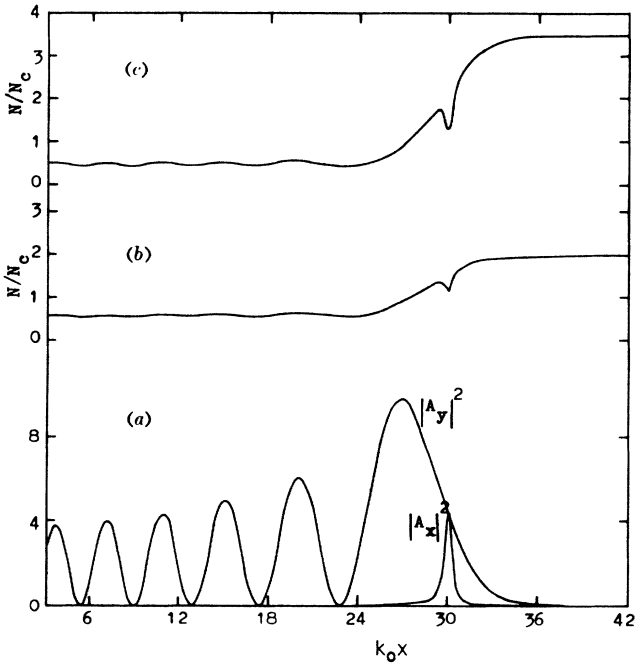

FIG. 2. The same as Fig. 1, but for $\sqrt{\alpha}=0.01$, $f=10^{-2}$.

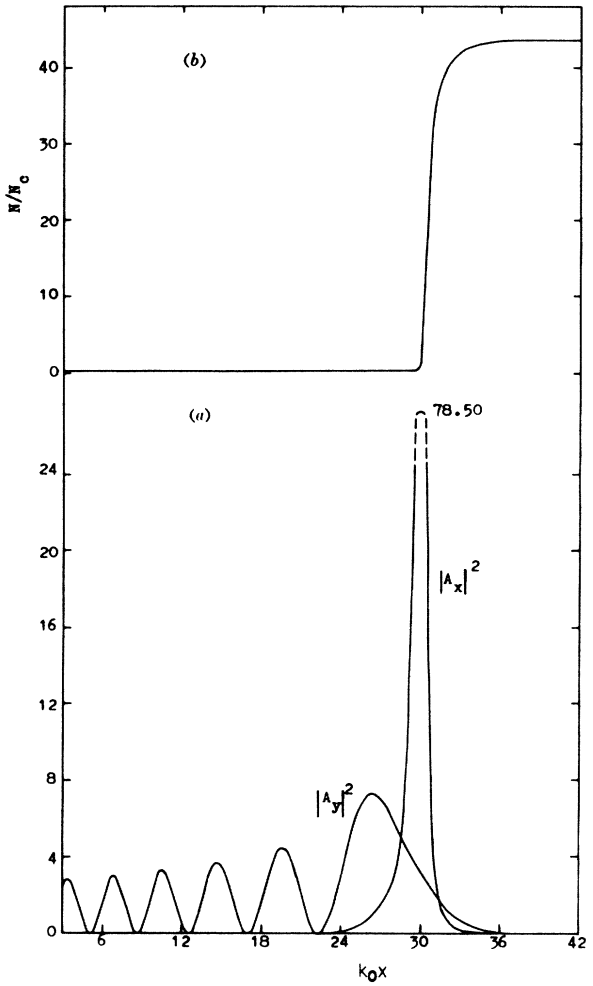

FIG. 3. The same as Fig. 1, but for $\sqrt{\alpha}=0.05$, $f=10^{-2}$.

vestigated the influence of the dc magnetic field on the field structure. Detailed results are shown in Figs. 1–3. It can be seen that A_x is always zero when $B_0=0$, and that the peak value of A_x increases as B_0 grows. Because the ponderomotive force is proportional to the amplitude gradient of the electric field, we could reasonably expect that the modification of plasma density caused by the ponderomotive force will be intensified under the influence of the magnetic field.

III. DENSITY-PROFILE STEEPENING

Knowing the electromagnetic field structure, we can further discuss the plasma-density modification by the ponderomotive force. It is well known that when laser light passes through a plasma with an initial linear density profile, the ponderomotive force pushes the electrons as well as the ions because of the quasineutral requirement of a plasma. As a result, a new density profile is formed where a balance between the force of the plasma pressure and the ponderomotive force has been reached, and the motion and density distribution of the plasma approach a steady state. At this time the behavior of the plasma can be described by the following fluid equations:

$$\frac{\partial}{\partial\xi}(NV)=0 , \tag{5}$$

$$V\frac{\partial V}{\partial\xi}=\frac{1}{4}\frac{v_0}{v_e}\frac{\partial A^2}{\partial\xi}-\frac{1}{N}\frac{\partial N}{\partial\xi} . \tag{6}$$

Equation (5) is the continuous equation and Eq. (6) the momentum equation. The time derivatives are set as zero because the plasma is considered to be in a steady state. All variables have been written in a dimensionless form, i.e., $\xi=k_0x$, $N=\omega_p^2/\omega^2$, $A=E/E_L$, $V=u/c_s$, where c_s is the ion sound speed, v_e the thermal velocity of the electron, $v_0=eE_L/m\omega$. The first term on the right-hand side of Eq. (6) represents the ponderomotive force, which is proportional to the spatial derivative of the electric fields.

Integrating Eq. (5) gives

$$NV=N_s , \tag{7}$$

where N_s is the integral constant which is equal to the plasma density at the sonic point ($V=1$). Equation (7) indicates that the product of density and velocity is a constant for all values of ξ. Solving Eq. (7) for N and then substituting it into Eq. (6), we have

$$\left[V-\frac{1}{V}\right]\frac{\partial V}{\partial\xi}=-\frac{1}{4}\frac{v_0^2}{v_e^2}\frac{\partial A^2}{\partial\xi} . \tag{8}$$

Since $\partial V/\partial\xi\neq 0$, A^2 reaches its maximum when $V=1$. There are a number of peaks in the intensity profile. The way we determine the sonic point is to choose the highest peak, which is responsible for the trans sonic flow.

Solving Eq. (7) for V and then substituting it into Eq. (6), we have another equation

$$\left[\frac{1}{N}-\frac{N_s^2}{N^3}\right]\frac{\partial N}{\partial\xi}=-\frac{1}{4}\frac{v_0^2}{v_e^2}\frac{\partial A^2}{\partial\xi} . \tag{9}$$

Integrating Eq. (9) gives

$$\frac{1}{2}\frac{N_s^2}{N^2}+\ln N=-\frac{1}{4}\frac{v_0^2}{v_e^2}A^2+\text{const} . \tag{10}$$

The constant in Eq. (10) is determined by applying the condition that the maximum A appears at the sonic point:

$$\text{const}=\frac{1}{2}+\ln N_s+\frac{1}{4}\frac{v_0^2}{v_e^2}A_s^2 , \tag{11}$$

where A_s is the field intensity at the sonic point.

From Eqs. (10) and (11) we obtain the elementary equation for density-profile calculation,

$$\left[\frac{N_s}{N}\right]^2+2\ln\frac{N}{N_s}-1=\frac{1}{2}\frac{v_0^2}{v_e^2}(A_s^2-A^2) . \tag{12}$$

Equation (12) is a transcendental equation which can be numerically solved if A is known. Before doing so we shall, at first, have a discussion about this equation.

Let $M=N/N_s$, then the left-hand side of Eq. (12) can be written as

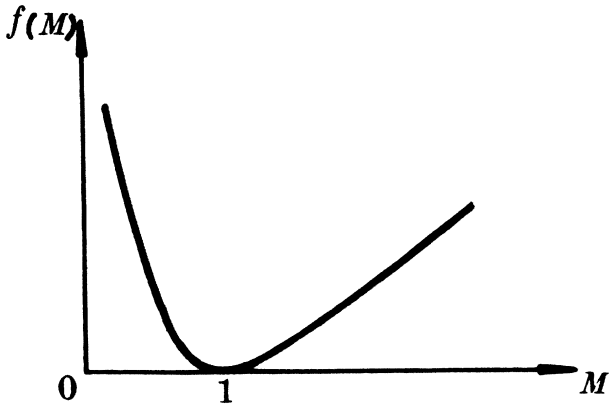

FIG. 4. The schematic behavior of function $f(M)$.

$$f(M)=\frac{1}{M^2}+2\ln M-1\ . \tag{13}$$

A plot of function $f(M)$ is shown in Fig. 4. We can see that $f(M)=0$ when $M=1$. It implies that $A=A_s$ according to Eq. (12). This is in agreement with the condition mentioned above that the field reaches its maximum at the sonic point. If $M\neq 1$, then $f(M)>0$; at this time Eq. (12) has two solutions which lie, respectively, on both sides of the sonic point. Since v_0^2 is proportional to the intensity of the incident light, it is easy to see that the more intense the incident laser light, the larger the value of $f(M)$ will be, and the more severe the density-profile steepening.

Besides the intensity of the incident light, the peak value of the field A_s is also closely related to the occurrence of resonance. The appearance of the resonance will generally lead to a significant increase of A_s. As previously mentioned, in a magnetized plasma, resonant effects will occur even when the laser light is normally incident. So it is obvious that the existence of a self-generated magnetic field will certainly play an important role in density-profile steepening.

In addition to the increase of A_s, resonance effects will result in a shift of the sonic point as well. This effect is clearly shown in Figs. 1 and 3. The sonic point is located somewhere ahead of the reflection surface (i.e., the critical density surface) when the dc magnetic field is absent, and it moves to the neighborhood of the critical surface when a large dc magnetic field is present.

Making use of the field structure obtained in Sec. II and Eq. (12) in this section, we have calculated the modified density profile over the whole coronal region. Typical results are illustrated in Figs. 1–3. The parameters used in the calculations are selected in accordance with the experimental observations so that our results can be compared with experiment.

IV. RESULTS AND DISCUSSION

Our computations show that besides the incident laser intensity, the density-profile modification depends significantly on the value of the parameter α. We can separate the effects of a self-generated field on the plasma-density modification into several cases.

(a) $\sqrt{\alpha}<0.01$. In this case, the dc magnetic field is so weak that though the resonant field A_x does not equal zero, it can still be neglected compared with A_y. So neither the value of A_s nor the position of the sonic point is significantly different from those when the dc magnetic field is absent. To illustrate the density profile for this case, we simply give the results in which B_0 is zero, as shown in Fig. 1. In comparing this with the initial linear density-profile distribution, we find profile steepening. For a light intensity of $v_0/v_e=0.4$–0.6, this corresponds to, assuming that the electron temperature is 1 KeV, $I_{\rm in}=8.8\times10^{14}$–$2\times10^{15}$ W/cm^2 for a Nd-glass laser and $I_{\rm in}=8.8\times10^{12}$–$2\times10^{13}$ W/cm^2 for a CO_2 laser, when the upper-shelf density is in the range of $(2$–$4)n_{\rm cr}$, and the lower-shelf density is about $0.5n_{\rm cr}$.

(b) $\sqrt{\alpha}\sim0.01$. The dc magnetic field in this case, though it is still not very strong, begins to manifest itself through resonance. The results are that A_s increases and that the sonic point has been relocated to the neighborhood of the critical surface. A characteristic of this case is a density dip that appears in the vicinity of the critical surface; see Fig. 2.

(c) $\sqrt{\alpha}>0.01$. When the value of the dc magnetic field is in this range, the resonant effects become more evident. Not only does the sonic point approach the critical surface, but A_s also becomes significantly large as the resonant peak rises sharply. As a result, the density profile close to the critical surface will be severely steepened. The upper-shelf density might reach above $10n_{\rm cr}$. If $\sqrt{\alpha}=0.05$, the upper-shelf density may reach as high as $40n_{\rm cr}$ and above, even if the intensity of incident light is only about 10^{13} W/cm^2 (CO_2 laser), as shown in Fig. 3. Such a high upper-shelf density is difficult to be interpreted by a nonmagnetized model.

The consistency of our computation with experiments is obvious. For Nd-glass laser beams at intensities 10^{15}–10^{16} W/cm^2, the self-generated magnetic field is up to 1 MG order,[13] i.e., $\sqrt{\alpha}\lesssim0.01$, corresponding to cases (a) and (b); the measured upper-shelf density is about $(1$–$4)n_{\rm cr}$,[3,4] in accordance with our results.

Although the analytic calculation and computer simulations without dc magnetic field considerations have presented similar results[7,10] for the upper-shelf density in the case of a Nd-glass laser, they have essential difficulties in explaining the results obtained in CO_2 laser target experiments.

For CO_2 laser beams at intensities 7×10^{12}–3×10^{14} W/cm^2, the self-generated magnetic field is in the range 100–500 kG,[14,15] i.e., $\sqrt{\alpha}=0.01$–0.05, corresponding to cases (b) and (c). The measured upper-shelf density ranges from $10n_{\rm cr}$ to $40n_{\rm cr}$.[5] This result, though far from being fully explained by the nonmagnetized model, is a natural consequence of our computations.

The density dip structure has been theoretically predicted for a number of situations.[16–19] The dips can result from momentum balance in both planar and spherical geometries as well as from caviton formation in the presence of obliquely incident p-polarized laser light. We here also mention a mechanism which is principally similar to that of the latter case, that is, the ponderomotive force

caused by the resonant field pushes the plasma aside in the vicinity of the resonant point, and hence induces a density dip. The difference is that our mechanism can operate even if the laser light is normally incident on an inhomogeneous plasma in the case of the presence of the self-generated dc magnetic field.

Finally, it should be pointed out that in this paper we have focused our discussion of the effects of the self-generated dc magnetic field on the density-profile modification. Therefore we pay much attention to the parameter α, but only set f to a fixed and reasonable value although the selection of f certainly has influence on the density-profile modifications. In addition, in this paper we have considered the plasma as collision dominated, and limited the intensity of the incident laser to below the threshold of wave breaking, so the effects of hot electrons could be neglected.

V. CONCLUSION

Our discussion demonstrates that the nonmagnetized plasma model can explain some of the observations in Nd-glass laser experiments only because the parameter α of this case is small enough so that the resonance induced by the self-generated magnetic field has not become dominant. We also suggest that magnetization effects should be taken into account in order to satisfactorily explain the observed phenomena of density-profile steepening either in CO_2 or in Nd-glass laser-plasma interaction experiments.

[1]C. E. Max, in *Laser-Plasma Interaction,* edited by Roger Balian and Jean-Claude Adam (North-Holland, Amsterdam, 1982), p. 301.
[2]W. L. Kruer, Bull. Am. Phys. Soc. **21**, 1648 (1976).
[3]D. T. Attwood, D. W. Sweeney, J. M. Auerbach, and P. H. Y. Lee, Phys. Rev. Lett. **40**, 184 (1978).
[4]A. Raven and O. Willi, Phys. Rev. Lett. **43**, 278 (1979).
[5]R. Fedosejevs, M. D. J. Burgess, G. D. Enright, and M. C. Richardson, Phys. Fluids **24**, 537 (1981).
[6]R. L. Carman, D. W. Forslund, and J. M. Kindel, Phys. Rev. Lett. **46**, 29 (1981).
[7]F. David, P. More, and R. Pellat, Phys. Fluids **26**, 747 (1983).
[8]K. G. Estabrook, E. J. Valeo, and W. L. Kruer, Phys. Fluids **18**, 1151 (1975).
[9]K. Lee, D. W. Forslund, J. M. Kindel, and E. L. Lindman, Phys. Fluids **20**, 51 (1977).
[10]Zhi-zhan Xu, Wei Yu, and Wen-qi Zhang, Bull. Am. Phys. Soc. **29**, 1325 (1984).
[11]R. B. White and F. F. Chen, Plasma Phys. **16**, 565 (1974).
[12]W. L. Kruer and K. Estabrook, Phys. Fluids **20**, 1688 (1977).
[13]A. Raven, P. T. Rumsby, J. A. Stamper, O. Willi, R. Illingworth, and R. Thareja, Appl. Phys. Lett. **35**, 526 (1979).
[14]N. A. Ebrahim, M. C. Richardson, R. F. Fedosejevs, and U. Feldman, Appl. Phys. Lett. **35**, 106 (1979).
[15]E. A. Mclean, J. A. Stamper, C. K. Mauka, H. R. Griem, D. W. Droemer, and B. H. Ripin, Phys. Fluids **27**, 1327 (1984).
[16]C. E. Max and C. F. McKee, Phys. Rev. Lett. **39**, 1337 (1977).
[17]J. Virmont, R. Pellat, and A. Mora, Phys. Fluids **21**, 567 (1978).
[18]R. D. Jones, C. H. Aldrich, and K. Lee, Phys. Fluids **24**, 310 (1981).
[19]C. H. Aldrich, R. D. Jones, and K. Lee, Phys. Fluids **27**, 2351 (1984).